Desalination and Water Treatment
www.deswater.com

doi: 10.5004/dwt.2021.27620

234 (2021) 136–146
September

Mechanism and efficiency of metronidazole removal via adsorption and heterogeneous Fenton reaction using $FeNi_3$ nanoparticles

Seyyedeh Masoomeh Rahimi[a], Tariq J. Al-Musawi[b], Fatemeh Sadat Arghavan[c], Negin Nasseh[d,*]

[a]*Student Research Committee, Birjand University of Medical Sciences, Birjand, Iran*
[b]*Department of Civil Engineering, Al-Qalam University College, Kirkuk, Iraq*
[c]*Student Research Committee, Department of Environmental Health Engineering, Faculty of Health, Mashhad University of Medical Sciences, Mashhad, Iran*
[d]*Social Determinants of Health Research Center, Department of Environmental Health Engineering, Faculty of Health, Birjand University of Medical Sciences, Birjand, Iran, Tel: +98-9197815053; email: negin_nasseh@yahoo.com*

Received 20 April 2021; Accepted 5 July 2021

ABSTRACT

Pharmaceutical wastewater is a source of many pollutants, the most important of which are antibiotics that can be toxic and carcinogenic to humans and animals. Therefore, finding a way to remove antibiotics from wastewater before discharging is of utmost importance by environmental researchers. In this study, the authors evaluated two widely used treatment methods which are adsorption and heterogeneous Fenton for metronidazole (MNZ) antibiotic removal. As an adsorbent and catalyst for the suggested processes, the $FeNi_3$ nanoparticles were applied. The application of $FeNi_3$ nanoparticles in the adsorption and heterogeneous Fenton processes achieved 45.09% and 100% MNZ antibiotic removal efficiencies, respectively. The effects study showed that the optimum conditions for removal are pH = 7 and 3 for adsorption and Fenton processes, respectively, reaction time = 180 min, MNZ antibiotic concentration = 10 mg/L, $FeNi_3$ nanoparticles dose = 0.005 g/L, and H_2O_2 concentration in Fenton process = 150 mg/L. The adsorption isotherm and kinetics data are consistent with the Langmuir isotherm and pseudo-second-order kinetic models, respectively. In addition, the kinetics data of MNZ antibiotic degradation using the heterogeneous Fenton process agreed with the pseudo-first-order reaction kinetics. It was found that the used $FeNi_3$ nanoparticles can be recycled five times in both processes with losses of less than 7% of MNZ antibiotic removal efficiencies from the first to fifth cycle.

Keywords: Adsorption; Heterogeneous Fenton; Metronidazole; Isotherm; Kinetics; Regeneration study

1. Introduction

Antibiotics are a class of drugs used to prevent and treat bacterial infections, with strong inhibitory 32 and lethal effects on bacteria, moulds, mycoplasma, and many other pathogenic microorganisms [1]. Compounds containing nitroaromatic groups are used to treat a wide variety of indications including Parkinson's disease, angina, and insomnia. Additionally, several nitroaromatics are used as anti-infective agents, including drugs to treat parasitic infections: for example, nitazoxanide is approved for giardiasis and cryptosporidiosis, metronidazole (MNZ) for trichomoniasis, giardiasis, and amoebiasis, and nifurtimox [2,3]. Nitroimidazole ($C_3H_3N_3O_2$) is a common antibiotic mainly applied to treat parasitic and anaerobic bacterial infections [4]. From the chemistry perspective, this antibiotic

* Corresponding author.

comprises three derivatives: MNZ, tinidazole, and nimorazole, where the first is the most produced by pharmaceutical factories [5]. MNZ is an antibiotic that has high activity against anaerobic bacteria and several types of protozoa. In addition, formulations containing MNZ have been used as safe medicines during pregnancy and lactation [6–8]. This antibiotic is on the WHO's List of Essential Medicines for humans [9]. The concentration of MNZ antibiotic in several samples taken from pharmaceutical wastewater has been reported to be 0.5 to 10 μg/mL [10]. In fact, the antibiotic residues are the main source of refractory micro-pollutants in the environment that they are present in notable concentrations in the liquid waste of pharmaceutical and care compounds industries. These residues are classified as highly toxic and carcinogenetic compounds, besides they resist the biodegradation processes, thus, they can cause great harm to water quality, aquatic life, animals, and eventually to human health [11]. The MNZ antibiotic has a ring structure which makes it potential to be carcinogenic and mutagenic by destroying the DNA of lymphocytes [12].

Therefore, it is critically necessary to find a treatment technology to properly remove the antibiotic pollutants from pharmaceutical wastewater prior to discharge into the environment. To achieve this goal, various techniques were tested to investigate their effectiveness and suitability in removing pharmaceutical compounds including antibiotics, such as advanced oxidation [13,14], ion exchange [15], activated carbon adsorption [16–18], membrane [19], biological purification [20], and ozonation [21]. Among the above-mentioned techniques, advanced oxidation processes (AOPs) have gained great interest in the treatment systems as this technology was found efficacious in the treating of pharmaceutical compounds laden wastewater [22–24]. AOPs are divided into photochemical and non-photochemical processes. The heterogeneous Fenton reaction process is one of the non-photochemical AOPs. The heterogeneous Fenton process is widely used to treat a large variety of water organic pollution such as pharmaceutical compounds, phenols, formaldehyde, dyes, pesticides, and rubber chemicals. The wide use of this process is due to its high efficiency in removing intractable elements in a relatively short operating time, relatively cheap, and its ability to mineralize the organic pollutants [25–28]. In addition, it does not required special equipment and there is no need for energy to activate hydrogen peroxide (H_2O_2). The mechanism of organic pollutant degradation by the Fenton method is based on the initial combination of H_2O_2 an oxidant agent and Fe^{2+} catalyst in an acidic media, as illustrated in the chemical reactions [Eqs. (1)–(7)] [26,29]. During these reactions, Fe^{2+} was rapidly oxidized by the strong oxidants (H_2O_2 and generated $^{\bullet}OH$ radicals) to Fe^{3+} ions [Eqs. (1) and (2)], while Fe^{2+} is regenerated through a so-called Fenton-like reaction that occurs between Fe^{3+} and H_2O_2 [Eq. (5)]. Eqs. (6) and (7) depict the resultant by-products from the Fenton method.

$$Fe^{2+} + H_2O_2 \rightarrow Fe^{3+} + {}^{\bullet}OH + OH^- \quad (1)$$

$$Fe^{2+} + {}^{\bullet}OH \rightarrow Fe^{3+} + OH^- \quad (2)$$

$$RH + {}^{\bullet}OH \rightarrow H_2O + R \rightarrow \text{further oxidation} \quad (3)$$

$$R^{\bullet} + Fe^{3+} \rightarrow Fe^{2+} + R^+ \quad (4)$$

$$Fe^{3+} + H_2O_2 \rightarrow Fe^{2+} + {}^{\bullet}OOH + H^+ \quad (5)$$

$$^{\bullet}OH + H_2O_2 \rightarrow {}^{\bullet}OOH + H_2O \quad (6)$$

$$^{\bullet}OH + {}^{\bullet}OH \rightarrow {}^{\bullet}OOH + OH^- \quad (7)$$

Nanomaterials have wide applications in different engineering fields, particularly in adsorption treatment systems of water and wastewater. This is because nanomaterials have high ability to remove many contaminants that are difficult to remove by conventional methods [30,31]. In this direction, using nanoparticles of magnetic properties as adsorbents has attracted great attention as simple and economical technology [32]. In fact, the application of magnetic nanoparticles in the treatment system facilitates their separation by the magnetic field and this helps in the disposal of these particles in easy and safe ways after treatment. More importantly, the separated magnetic nanoparticles can be recycled, and no hazardous wastes are generated during treatment processes. Currently, widely used magnetic nanoparticles as a treatment agent include $FeNi_3$ nanoparticles. This is because of their high electromagnetism value, and most importantly, they are non-toxic materials [33,34]. Given the good reputation that $FeNi_3$@ nanoparticles have in the field of treatment systems of pharmaceutical wastewater, the ability of these nanoparticles for MNZ antibiotic removal was not previously investigated. Therefore, in this study, $FeNi_3$ nanoparticles were initially synthesized and then applied as a treatment agent for the removal of MNZ antibiotic from wastewater using adsorption and heterogeneous Fenton processes. The mechanism of MNZ antibiotic removal in both processes, effects of operational parameters, kinetic and adsorption processes were studied.

2. Materials and methodology

2.1. Materials

The MNZ of a powder form (purity > 99.9%) was purchased from Sigma Aldridge Co. (Germany). The MNZ working solutions were prepared via dissolving appropriate weights of MNZ using distilled water. Table 1 is listed in the physiochemical properties of the used MNZ antibiotics. The $FeNi_3$ nanoparticles were synthesized using the following chemicals: polyethylene glycol (PEG, $C_{2n}H_{4n+2}O_{n+1}$), iron chloride ($FeCl_2.4H_2O$), nickel chloride ($NiCl_2.6H_2O$), hydrazine hydrate ($N_2H_4.H_2O$), ethanol (C_2H_5OH), all purchased from Merck (Germany). In this study, the H_2O_2 was used as an oxidizing agent. In addition, HCl and NaOH solutions (0.2 M) were used for pH adjustment of working solutions (Merck, Germany), using a pH-meter (Knick 761 pH meter, Calimatic).

2.2. Methods

2.2.1. Synthesis of $FeNi_3$ nanoparticles

To synthesis $FeNi_3$ nanoparticles, the following experimental steps of the co-precipitation process were adopted

Table 1
Physiochemical properties of metronidazole (MNZ) antibiotic used in this study

Property	Value
Molecular formula	$C_6H_9N_3O_3$
Molecular weight	171.20 g/mol
p*Ka* value	2.55
Solubility in water	9.50 g/L
Molecular structure	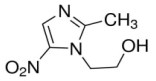

(1, 21): first, 2 g of PEG was dissolved in 300 mL deionized water. Next, 0.6 g of $FeCl_2.4H_2O$ and 1.4 g of $NiCl_2.6H_2O$ were separately dissolved in 30 mL deionized water and poured into a pre-prepared PEG solution. The pH value of the mixture was set at a range of 12 to 13 by dropwise addition of HCl or NaOH. Then, 27 mL of $N_2H_4.H_2O$ (concentration 80%) were mixed with the obtained solution at 150 rpm for 24 h, where the pH value of this mixture was also controlled at 12–13. At the end of this reaction, $FeNi_3$ nanoparticles as a black precipitate was formed, which withdraw using N42 magnet, washed with deionized water, and finally dried at 75°C before being applied in the adsorption and heterogeneous Fenton processes.

2.2.2. Experimental work

The experiments of MNZ antibiotics adsorption and degradation were conducted in a batch system using a 1-L opaque flask at the laboratory temperature. Initially, the MNZ stock solution of concentration 100 mg/L was prepared by dissolving a specific amount of MNZ antibiotic powder in deionized water. Afterwards, the working solutions at different concentrations were prepared by dilution. It is worth mentioning that all the prepared MNZ antibiotic solutions were kept in the darkness at 4°C in order to avoid the interaction of MNZ antibiotics with light and used for one week at most. A magnetic mixer (Agitateur magnétique chauffant 10 L – DC180 – Froilabo) was used to mix solutions at 350 rpm. Both processes were conducted at the following conditions: pH (3–11), $FeNi_3$ nanoparticle dose (0.005–0.1 g/L), initial MNZ antibiotic concentration (10–30 mg/L), reaction time (0–180 min), and H_2O_2 concentration in the Fenton process (100–200 mg/L). Samples of 2 mL were sucked with a syringe at different intervals of reaction time and the remaining MNZ antibiotics concentration was determined by a UV/VIS spectrophotometer (T80$^+$ UV/Visible, PG Instruments Ltd) at a 320 nm spectral peak [35]. The removal efficiency was determined by comparing the initial and remaining MNZ antibiotic concentrations. Notably, for the samples taken from the Fenton flask, a 200 μL of 0.2% $Na_2S_2O_3$ normal solution was added to these samples immediately after being taken to minimalize the interventional effect of H_2O_2. Once the adsorption or Fenton reaction is over, $FeNi_3$ nanoparticles are magnetically separated from the solution and the total quantity is collected in a container to be prepared for the regeneration tests. Each sample was tested three times in the UV/VIS spectrophotometer where the average value was taken in the calculations. The removal efficiency [R(%)] of $FeNi_3$ nanoparticles for MNZ antibiotic were determined using Eq. (8):

$$\mathrm{RE}(\%) = \frac{(C_0 - C_t)}{C_0} \times V \tag{8}$$

where C_0 and C_t are the measured MNZ antibiotic concentrations (mg/L) before the adsorption/Fenton process and after a specific period of the treatment process (t, min), respectively.

In addition, Eq. (9) is used to determine the adsorption capacity (q_t) which is an essential parameter in the adsorption study to evaluate the adsorption of pollutants by the used adsorbent. Notably, the concentration and adsorption capacity at adsorption equilibrium time is denoted by C_e (mg/L) and q_e (mg/g), respectively.

$$q_t = \frac{C_0 - C_t}{M/V} \tag{9}$$

where M/V denotes the used adsorbent dose (g/L) in the contaminated solution [36].

2.2.3. Isotherm and kinetics of adsorption

For this study, an experiment was performed to determine the relationship between adsorption capacity values [Eq. (9)] of $FeNi_3$ nanoparticles for MNZ antibiotic concentration at equilibrium status (contact time = 120 min). On another side, the results of the effects of MNZ antibiotic concentration at different contact times were used for the kinetic study. The well-known Langmuir and Freundlich isotherm models were used to fit the isothermal data of equilibrium adsorption of MNZ antibiotic onto $FeNi_3$ nanoparticles. The Langmuir model [Eq. (10)] is used to modeling of mono-layer isotherm adsorption, which means each pollutant molecule interacts with one site located on the adsorbent surface. In addition, the used adsorbent has a homogenous adsorption site of limited capacity toward pollutant adsorption [27,37,38].

$$\frac{C_e}{q_e} = \frac{1}{q_m K_L} + \frac{C_e}{q_m} \tag{10}$$

where q_m (mg/g) is a Langmuir model parameter denoting the maximum adsorption capacity of the used adsorbent, and K_L (L/mg) is an equilibrium constant that reflects the affinity level of adsorption sites of the adsorbent used for adsorption of target pollutant from aqueous solution.

In addition, the characteristic of the adsorption process using Langmuir isotherm can be defined based on the dimensionless separation factor (R_L) [Eq. (11)]. Based on this factor value, the favorable adsorption case can be only diagnosed at $0 < R_L < 1$.

$$R_L = \frac{1}{(1 + K_L C_0)} \tag{11}$$

The Freundlich equation [Eq. (12)] is an empirical isotherm formula that is generally used, unlike the Langmuir model, to describe the multi-layer and heterogeneous adsorption systems [37,39].

$$\log q_e = \frac{1}{n}\log C_e + \log K_F \tag{12}$$

where K_F is a parameter associated with binding energy, and $1/n$ is the heterogeneity parameter.

In addition, the experimental data of Fig. 3b were first treated using Eq. (9) and then analyzed in terms of pseudo-first-order [Eq. (13)] and pseudo-second-order [Eq. (14)] equations of kinetics adsorption [40].

$$\log\left(q_e - q_t\right) = \log q_e - \frac{K_1}{2.303}t \tag{13}$$

$$\frac{t}{q_t} = \frac{1}{K_2 q_e^2} + \frac{t}{q_e} \tag{14}$$

where K_1 (1/min) and K_2 (g/mg min) are the rate constants, respectively, and t is the adsorption time (min).

3. Result and discussion

3.1. Effect of pH on the MNZ antibiotics removal efficiency

The effect of solution pH on the adsorption and degradation efficiency for MNZ antibiotic removal by $FeNi_3$ nanoparticles was investigated at pH = 3, 5,7, 9, and 10. The other experimental parameters were fixed at reaction time = 60 min, $FeNi_3$ nanoparticles dose = 0.02 g/L, and MNZ antibiotic concentration = 20 mg/L, and H_2O_2 concentration in Fenton process = 150 mg/L. The results of this experiment were depicted in Fig. 2. The highest values for MNZ antibiotic removal via adsorption (Fig. 2a) and degradation (Fig. 2b) processes were recorded at pH 7 and pH 3, respectively. The results depicted from the adsorption process (Fig. 2a) can be reasoned based on the nature and valance of both adsorbent surface and pollutant molecule at a specific pH value. In this direction, the pHpzc is a useful parameter to indicate the surface charge type (positive or negative) of an adsorbent as a function of pH [27]. Notably, the experiment for this parameter was conducted depending on the detailed steps mentioned in Mohseni-Bandpei et al. [39]. Accordingly, the pHpzc of a sample of $FeNi_3$ nanoparticles was determined to be 6.7 as shown in Fig. 1c. This means that $FeNi_3$ nanoparticles will have a positive charge at a solution pH < 6.7 and vice versa. From another side, it is known that the dissociation constant defined by the pKa value of MNZ antibiotic molecules is 2.55 (Fig. 1d). However, the MNZ-H^+ will be the surplus speciation form of the MNZ antibiotic molecule in an acidic medium [43,44]. As a result, the solution pH < pHpzc, a high repulsive rate between the adsorbent particle and pollutant molecules will be occurred. This phenomenon, in fact, restricts the adsorption of MNZ antibiotic molecules onto $FeNi_3$ nanoparticles; consequently, the removal efficiency of MNZ antibiotic was decreased when the solution being more acidic. At neutral pH, the repulsive force almost non-existent. Thus, the MNZ molecules will have a high tendency to be adsorbed $FeNi_3$ nanoparticles. This will promote MNZ antibiotic removal efficiency via the adsorption process. At pH > 7, the adsorbent particles will have negative charges as this pH value > pHpzc. In addition, the MNZ molecule at alkaline medium will be of MNZ-OH^- form. Under these circumstances, the repulsive force between the MNZ-OH^- and negatively charged $FeNi_3$ nanoparticles will be high, leading to a low adsorption rate. In the heterogonous Fenton process, where H_2O_2 was added in this experiment with concentration = 150 mg/L, the degradation rate of MNZ molecules was high at acidic medium (Fig. 2b). This is due to the hydration of the catalyst surface by surplus H^+ at acidic pH values. This will promote the adhering of the MNZ molecules of the anionic form,that is, MNZ-OH^-. Thus, high reaction rate produces high removal rate via degradation reactions. Another reason is the conversion of the surplus H^+ to H^- radicals in acidic solutions. As a result, the increase of these strong radicals in high concentration in the aqueous solution will enhance the degradation activity of the used catalyst in the Fenton process which will intensify the degradation rate of the organic pollutants. Hence, high removal efficiency of MNZ antibiotic was determined at pH = 3. From another side, catalyst surface is negative at amounts of pH more than pH_{ZPC} and hydroxide groups

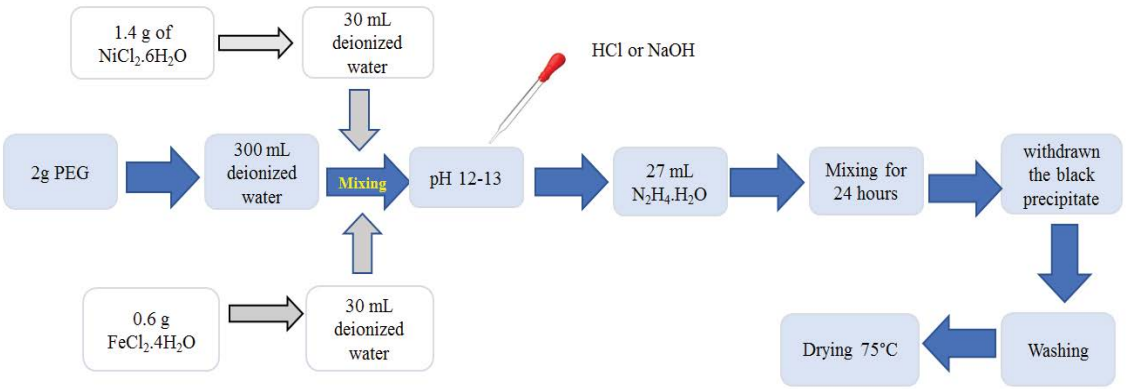

Fig. 1. Schematic of $FeNi_3$ nanoparticles synthesis.

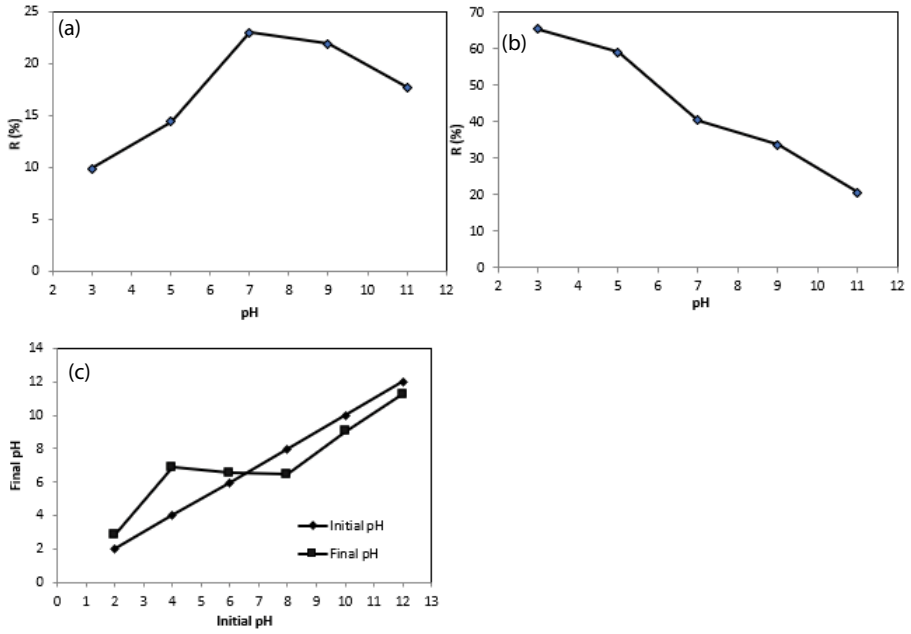

Fig. 2. Effect of pH value on MNZ antibiotic removal efficiency using adsorption process (a) and heterogeneous Fenton process (b), and pH_{pzc} analysis (c).

on it are deprotonated and produce OH^-. Ionized iron in this structure may combine with OH^- groups and result in Ferrous oxide sediment and as a result, does not allow to absorb sites. Moreover, the catalytic ability of $FeNi_3$ decreases due to a decrease in hydroxyl radical in alkali media. Thus, contaminant removal percent decreases at these amounts of pH due to its adsorption on nanocatalyst surface and proton deficiency stops Fenton reaction. The surface charge of $FeNi_3$ is positive at a pH lower than pH_{ZPC}. In these conditions, H^+ contained in solutions promotes hydroxyl groups at the surface of this catalyst and as a result, the catalyst surface goes to be more hydrated. Moreover, hydroxyl groups start to sediment at pH more than 4 and H_2O_2 forms oxonium ion at pH lower than 2 which is its oxidation power is very higher and is more stable. Hydroxyl ion discharge increases by H^+ at pH lower than 2 which affects degradation efficiency. The reaction system will face a change in iron concentration when pH goes from acidic to neutral and alkali form, such that oxidation concentration of Fe (Fe^{2+}) decreases in these media and thus, intervenes catalyst activity [43]. Results given from Hu et al. [1] and Rahmatinia [44] studies are consistent with current research [1,44]. From this experiment, one can deduce that the pH value and thus the rate of attraction between the $FeNi_3$ nanoparticles particles and the MNZ molecules have a major role in the removal process in both adsorption and Fenton processes.

3.2. Effect of $FeNi_3$ dose

The effect of $FeNi_3$ nanoparticles dose on the adsorption and degradation processes of MNZ antibiotic is shown in Fig. 3a and b. The conditions at which this experiment was conducted were: pH = 7 and 3 for adsorption and Fenton processes, respectively, reaction time = 0–180 min, $FeNi_3$ nanoparticles dose = 0.005–0.1 g/L, MNZ antibiotic concentration = 20 mg/L, and H_2O_2 concentration in Fenton process = 150 mg/L. For adsorption processes, when the catalyst dose increased, the removal efficiencies of MNZ antibiotic were also increased. This is due to the increase of the active site number as a result of an increase of catalyst dose. In contrast, the increase of $FeNi_3$ dose from on MNZ antibiotic 0.05 to 0.1 g/L had a negative effect on the MNZ antibiotic removal efficiency. In reality, this finding may be the outcome of turbidity increase as a result of the agglomeration of some of the $FeNi_3$ particles. This increase in turbidity means that the surface reaction sites will reduce. Comparison of the two figures it can be seen that the Fenton process has a more powerful activity for MNZ antibiotic removal than the adsorption process, and this is an evidence of the important role of H_2O_2 play in the MNZ antibiotic removal process.

3.3. Effect of MNZ antibiotic concentration on its removal efficiency

The effects of the variation of MNZ antibiotic concentrations on its removal efficiency by the adsorption and heterogeneous Fenton process are shown in Fig. 4. This experiment was conducted under conditions: pH = 7 and 3 for adsorption and Fenton processes, respectively, reaction time = 0–180 min, $FeNi_3$ nanoparticles dose = 0.005 g/L, and H_2O_2 concentration in Fenton process = 150 mg/L. Clearly, the MNZ antibiotic removal percent increases in both processes with an increase in MNZ antibiotic initial concentration, such that the highest removal percent is seen at the initial concentration = 10 mg/L and the lowest removal percent is seen at 30 mg/L. In the adsorption process (Fig. 4a), the removal efficiency of MNZ antibiotic was decreased from 45.09% to 27.09% with the initial

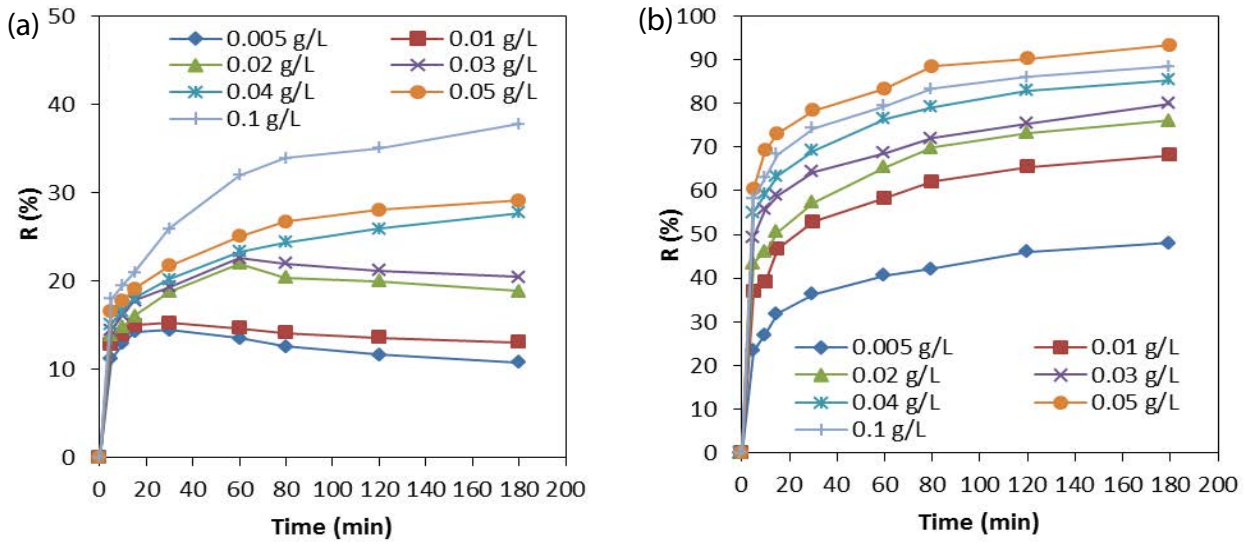

Fig. 3. Effect of $FeNi_3$ dose on the MNZ antibiotic removal efficiency using adsorption process (a), and heterogeneous Fenton process (b).

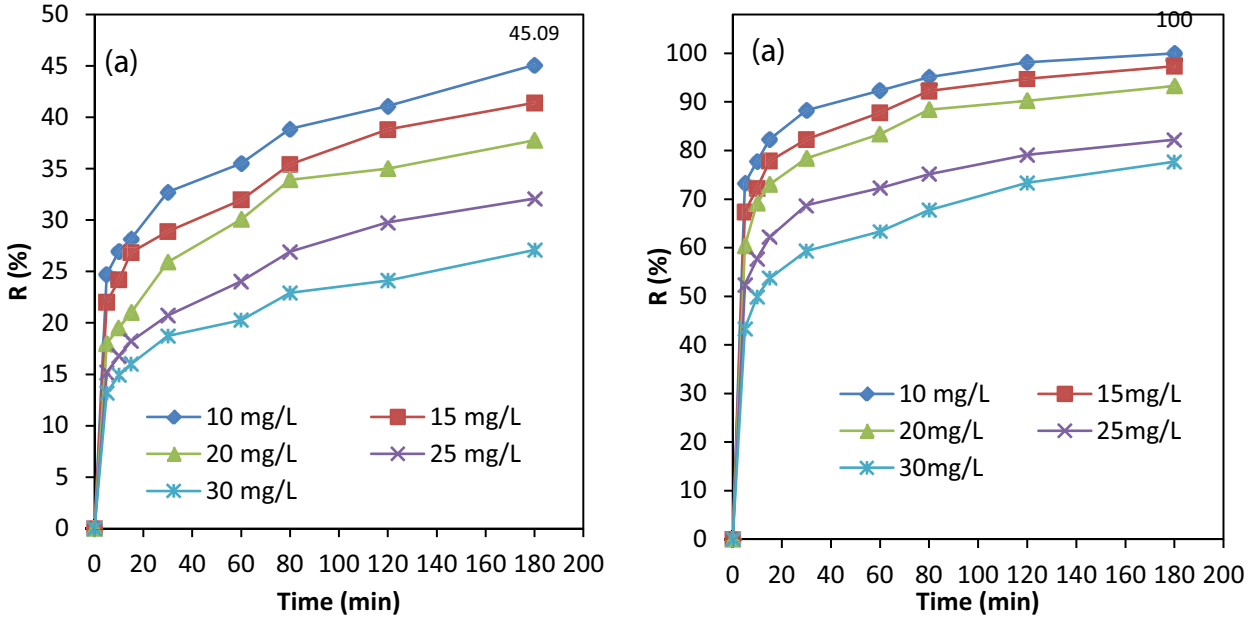

Fig. 4. Effect of MNZ antibiotic concentration on its removal efficiency using adsorption process (a), and heterogeneous Fenton process (b).

concentration decreased from 10 to 30 mg/L. This is due to that for all MNZ antibiotic concentration range, the used quantity of adsorbent is fixed. This means that when the pollutant concentration increased in an aqueous solution, the competition among its molecules will intensify for the available sites for the adsorption. As a result of this phenomenon, the available sites (onto the surface of $FeNi_3$ nanoparticles) will be quickly saturation at high concentrations of MNZ antibiotic [45,46]. At low pollutant concentrations, the ratio of the number of active sites to the MNZ molecules is low and thus high removal efficiency was determined. From this experiment, it can be concluded that the MNZ antibiotic removal efficiency in the adsorption process was highly dependent on its concentration in the aqueous solution. In the Fenton process, it was achieved a 100% of MNZ antibiotic degradation of 10 mg/L concentration and at a 180 min reaction time. While the degradation process was above 77% in the case of MNZ antibiotic concentration = 30 mg/L (Fig. 4b). This is because the amount of catalyst and H_2O_2 concentration are fixed for both concentration values thus the amount of hydroxyl radical produced in the Fenton process is the same. Therefore, the degradation efficiency will

more at low concentration since the percentage of hydroxyl radicals number to MNZ molecules will be high at low MNZ antibiotic concentration and vice versa [47].

From another side, Figs. 3 and 4, also indicated that the removal efficiency was rapid so that it significantly increased by more than 55% in the first 20 min adsorption/degradation time. Then, it was reached to equilibrium at 120 min. In reality, the rapid removal property for $FeNi_3$ nanoparticles is a desirable feature and favorable practical utility in the suggested treatment and it usually results from the abundance of reaction sites on the surface of the used adsorbent/catalyst at the beginning of the reaction.

3.4. Effect of H_2O_2 concentration added in Fenton process

Effect of H_2O_2 concentration (50–200 mg/L) on catalytic Fenton was examined in the following conditions: pH = 3, reaction time = 0–180 min, and $FeNi_3$ nanoparticles dose = 0.005 g/L. It is worth mentioning that the H_2O_2 should be carefully selected according to in according to the type and concentration of the contaminant. Various studies show that adding H_2O_2 in most cases results in increased oxidation in Fenton catalytic processes. However, as can be seen in Fig. 5, the efficiency of MNZ antibiotic removal increases with increasing H_2O_2 concentration from 50 to 150 mg/L and decreases at 200 mg/L. It is worthy to mention that H_2O_2 concentration is a key factor in the degradation of organic materials in advanced oxidation processes including heterogeneous Fenton reaction, as this agent is responsible for the production of oxidizing radicals via the reactions illustrated in the following equations [48].

$$H_2O_2 + e^- \rightarrow OH^- + OH^\bullet \quad (15)$$

$$H_2O_2 + O_2^{\bullet -} \rightarrow OH^\bullet + OH^- + O_2 \quad (16)$$

From another side, by increasing H_2O_2 concentration more than 150 mg/L, the performance of heterogeneous Fenton for MNZ antibiotic degradation has clearly reduced.

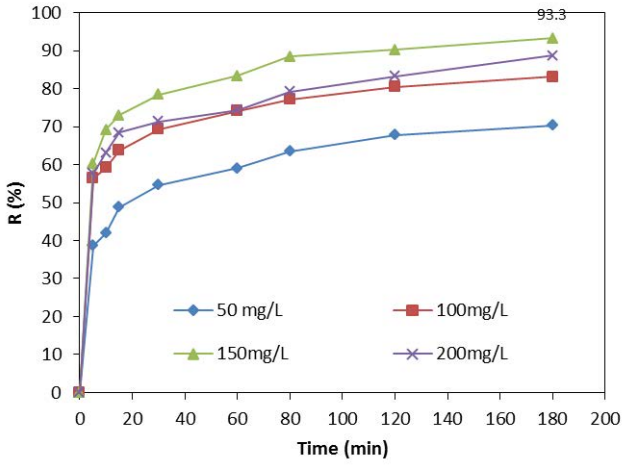

Fig. 5. Effect of H_2O_2 concentration on MNZ antibiotic degradation in heterogeneous Fenton process.

This may be due to the overreaction of H_2O_2 with $OH^\bullet$ radicals and the formation of HO_2 radicals as shown in Eqs. (17) and (18) [49].

$$OH^\bullet + H_2O_2 \rightarrow H_2O + HO_2^\bullet \quad (17)$$

$$H_2O_2 + h^+ \rightarrow H^+ + HO_2^\bullet \quad (18)$$

Prados et al. [50] studied the photodegradation process efficiency in MNZ antibiotic removal using ultraviolet radiation. The results of this study revealed that removal efficiency decreases by increasing H_2O_2 concentration. In addition, similar results were obtained in Nasseh et al. study [48].

3.5. Isotherm and kinetics of adsorption

The kinetics results of the MNZ antibiotic adsorption onto $FeNi_3$ nanoparticles analysis are listed in Table 2. Results showed that high regression values were obtained for the pseudo-second-order model, in contrast with pseudo-first-order results. Additionally, the values of q_e (cal) of the pseudo-second-order were close to the q_e (exp) values. In reality, these results indicating chemisorption reactions of the MNZ antibiotic molecules and $FeNi_3$ nanoparticles [1,51].

Table 2 lists the results of the determined constants of each isotherm model and coefficient of determination (R^2). The highest R^2 values were found for the Langmuir model; indicating that each MNZ molecule will be adsorbed onto one active site of $FeNi_3$ nanoparticles (mono-layer adsorption). In addition, the maximum adsorption capacity of $FeNi_3$ nanoparticles for MNZ antibiotic based was 131.58 mg/g. Based on the determined R_L values of the Langmuir model, which is between zero and one, the adsorption process of MNZ antibiotic onto $FeNi_3$ nanoparticles is determined to be favorable. Results of the Freundlich model showed that the adsorption process is referred to be desirable, as the value of the parameter n is greater than one.

3.6. Kinetics study of degradation

To study the kinetics process of the MTZ degradation, the applied pseudo-first-order kinetics model of the degradation process [Eq. (19)] was fitted with the experimental degradation data depicted in Fig. 3b. In fact, this model is proposed as the most suitable formula to describe the experimental kinetic data of degradation pollutants using the Fenton process [27,51].

$$\ln\left(\frac{C_t}{C_0}\right) = -k_{obs}t \quad (19)$$

Table 3 lists the results of the kinetics analysis including the rate constant of the pseudo-first-order model (k_{obs}, min^{-1}), half-life time corresponding to 50% MTZ degradation efficiency ($t_{50\%}$, min), and coefficient of determination (R^2) values. The k_{obs} values were found from the linear plot of $\ln(C_t/C_0)$ and irradiation time (t min), and $t_{50\%}$ is equal to = $0.693/k_{obs}$ [25]. The R^2 values in the studied

range of MTZ antibiotic concentration (10–30 mg/L) were found to be high (>0.93); thus, the degradation kinetics data of MTZ in heterogeneous Fenton treatment process using $FeNi_3$ nanoparticles is highly consistent with pseudo-first-order kinetics. Furthermore, the rate constant values were decreased with the increase in the MNZ antibiotic concentration. This reduction is a result of the generation of intermediate byproducts during MNZ antibiotic degradation, which prevent reaction of MNZ molecules with the active hydroxyl radicals, thus lowering the rate constant.

3.7. Regeneration study

The reusability of a treatment agent (adsorbent or catalyst) is an important parameter related to the cost of the treatment system [52,53]. In the present study, the recyclability of the $FeNi_3$ nanoparticles was tested for five consecutive cycles of MNZ antibiotic adsorption and degradation in the Fenton process. This experiment was performed under optimal conditions for each process: pH = 7 and 3 for adsorption and Fenton process, respectively, reaction time = 180 min, $FeNi_3$ nanoparticles dose = 0.005 g/L, MNZ antibiotic concentration = 10 mg/L, and H_2O_2 concentration in Fenton process = 150 mg/L. At the end of each adsorption/heterogeneous Fenton process cycle, the used quantity of $FeNi_3$ nanoparticles was withdrawn from the MNZ antibiotic solution using N_{42} magnet, rinsed with ethanol and deionized water to remove the attached MNZ molecules onto $FeNi_3$ nanoparticles, dried overnight at 70°C, and then reused in the next adsorption/degradation cycle. The results depicted in Fig. 6 indicating that the $FeNi_3$ nanoparticles can be recycled to a greater degree in the adsorption process than in the Fenton process. Such results may be due to the loss of activity of some $FeNi_3$ nanoparticles during the degradation reactions, while the adsorption process did not lead to damage in the adsorbent's active groups responsible for the MNZ antibiotic adsorption from the aqueous solution. In addition, the used $FeNi_3$ nanoparticles can be regenerated and reused five times in both treatment processes with only slight losses in their activity (<7%).

Table 2
Isotherm and kinetics models parameters of MNZ antibiotic adsorption onto $FeNi_3$ nanoparticles

Isotherm models						
Langmuir				Freundlich		
q_m	K_L	R^2	R_L	K_F	n	R2
131.58	0.083	0.09973	0.38	18.08	1.92	0.9589
Kinetics models						
Pseudo-first-order			Pseudo-second-order			
q_e (cal)	k_1	R^2	q_e (cal)	k_2	R^2	q_e (exp)
8.36	0.0179	0.96	144.93	0.0366	0.99	150.23

4. Conclusion

In the present research, $FeNi_3$ nanoparticles were prepared by the coprecipitation process and then applied as an adsorbent in the adsorption system and catalyst in the heterogeneous Fenton reaction to eliminate MNZ antibiotic from the contaminated solution. It was found that the heterogeneous Fenton process was more powerful to degrade the MNZ molecules than the adsorption process. From the results, the maximum removal efficiencies achieved in the adsorption and heterogeneous Fenton process were 45.09% and 100%, respectively, at the optimized conditions (pH = 7 and 3 for adsorption and Fenton processes, respectively, reaction time = 180 min, $FeNi_3$ nanoparticles dose = 0.005 g/L, MNZ antibiotic

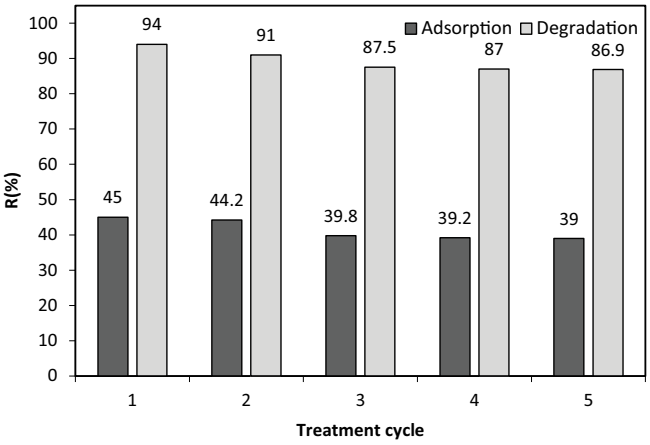

Fig. 6. Regeneration and recycling analysis of $FeNi_3$ nanoparticles for MNZ antibiotic removal via adsorption, and heterogeneous Fenton process.

Table 3
Kinetics of the MNZ antibiotic degradation in heterogeneous Fenton process using $FeNi_3$ nanoparticles

MNZ concentration (mg/L)	k_{obs} (min^{-1})	$t_{50\%}$ (min)	R^2	Equation of the linear plot, where $Y = \ln(C/C_0)$ and $x = t$
10	2.21×10^{-3}	31.35	0.9893	$Y = 0.0221x + 1.3167$
15	1.41×10^{-3}	49.15	0.9803	$Y = 0.0141x + 1.2314$
20	0.96×10^{-3}	72.18	0.9318	$Y = 0.0096x + 1.1409$
25	0.53×10^{-3}	130.75	0.9379	$Y = 0.0053x + 0.8821$
30	0.50×10^{-3}	138.60	0.9490	$Y = 0.0050x + 0.6721$

concentration = 10 mg/L, and H_2O_2 concentration in Fenton process = 150 mg/L). The results of the isotherm study showed that the Langmuir model has been found to be the best fit model for the adsorption isothermal data with the maximum uptake = 131.58 mg/g. Additionally, the kinetics data revealed that the MNZ antibiotic adsorption occurred through chemical reactions as the kinetics data followed well the pseudo-second-order reaction. From another side, kinetics data of MNZ antibiotic degradation in the heterogeneous Fenton process followed pseudo-first-order reaction kinetics. The regeneration study demonstrated that the $FeNi_3$ nanoparticles can be recycled to a greater degree in the adsorption process than in the Fenton process. In addition, these nanoparticles can be regenerated and reused five times in both treatment process with only slight losses in its removal efficiency for MNZ antibiotic (<7%). From this study, it was found that the $FeNi_3$ nanoparticles are an active catalyst for MNZ antibiotic removal and, thus, it is recommended to apply it in the heterogeneous Fenton process for the treatment of pharmaceutical wastewater, including MNZ antibiotic. Also, it is suggested to apply $FeNi_3$ nanoparticles as an adsorbent in the adsorption process which is can be installed as a complementary process for the btreatment of pharmaceutical wastewater.

Acknowledgments

Authors acknowledge the Birjand University of Medical Sciences for providing financial and scientific support to this research with the ethical code of IR.BUMS.REC.1399.293.

CRediT Authorship Contribution Statement

Seyyedeh Masoomeh Rahimi: Writing and discussion. Tariq J. Al-Musawi: Writing, software, and editing. Fatemeh Sadat Arghavan: Writing and discussion. Negin Nasseh: Editing, discussion, and supervision.

Funding

The Birjand University of Medical Sciences has provided financial support for this research.

Availability of data and materials

All data generated or analyzed during this study are included in this article.

Compliance with ethical standards

Competing interests

The authors of this paper affirm that they do not have any financial interest or personal relationship, which might influence themselves.

Consent to participate

Not applicable.

Consent to publish

Not applicable.

Conflict of interest

On behalf of all authors, the corresponding author states that there is no conflict of interest.

References

[1] Y. Hu, G. Wang, M. Huang, K. Lin, Y. Yi, Z. Fang, P. Li, K. Wang, Enhanced degradation of metronidazole by heterogeneous sono-Fenton reaction coupled ultrasound using Fe_3O_4 magnetic nanoparticles, Environ. Technol., (2017) 1–22, doi: 10.1080/09593330.2017.1374470.
[2] S.R Wilkinson, C. Bot, J.M Kelly, B.S Hall, Trypanocidal activity of nitroaromatic prodrugs: current treatments and future perspectives, Curr. Top. Med. Chem., 11 (2011) 2072–2084.
[3] S. Patterson, S. Wyllie, Nitro drugs for the treatment of trypanosomatid diseases: past, present, and future prospects, Trends Parasitol., 30 (2014) 289–298.
[4] N. Nasseh, B. Barikbin, L. Taghavi, M.A. Nasseri, Adsorption of metronidazole antibiotic using a new magnetic nanocomposite from simulated wastewater (isotherm, kinetic and thermodynamic studies), Compos. B. Eng., 159 (2019) 146–156.
[5] A. Mital, Synthetic nitroimidazoles: biological activities and mutagenicity relationships, Sci. Pharm., 77 (2009) 497–520.
[6] C.F. Rediguieri, V. Porta, D.S. Nunes, T.M. Nunes, H.E. Junginger, S. Kopp, K.K. Midha, V.P. Shah, S. Stavchansky, J.B. Dressman, Biowaiver monographs for immediate release solid oral dosage forms: metronidazole, J. Pharm. Sci., 100 (2011) 1618–1627.
[7] N. Okhovat, M. Hashemi, A. Golpayegani, Photocatalytic decomposition of metronidazolein aqueous solutions using titanium dioxide nanoparticles, J. Mater. Environ. Sci., 6 (2015) 792–799.
[8] H. Azarpira, Y. Mahdavi, O. Khaleghi, D. Balarak, Thermodynamic studies on the removal of metronidazole antibiotic by multi-walled carbon nanotubes, Der Pharmacia Lettre, 8 (2016) 107–113.
[9] F. Azadbakht, A. Esrafili, M. Yeganeh Badi, J. Sajedifar, M. Amiri, M. Gholami, Efficiency of persulfate-based advanced oxidation process ($UV/Na_2S_2O_8$) in removal of metronidazole from aqueous solutions, JMUMS, 27 (2017) 119–129.
[10] M. Kermani, A.F. Bahrami, A. Esrafili, M. Farzadkia, A.S. Salahshur, Identification of oxidation intermediates and investigation of toxicity changes in heterogenic catalytic ozonation process in the presence of MgO nanoparticles for metronidazole removal from aqueous solution, Health Syst. Res., 13 (2016).
[11] D. Balarak, F.K. Mostafapour, Photocatalytic degradation of amoxicillin using UV/synthesized NiO from pharmaceutical wastewater, Indones. J. Chem., 19 (2019) 211–218.
[12] I. Nasseh, M. Khodadadi, R. Khosravi, A. Beirami, N. Nasseh, Metronidazole removal methods from aquatic media: a systematic review, Ann. Mil. Health Sci. Res., 14 (2016) e13756, doi: 10.5812/amh.13756.
[13] B. Kamarehie, A. Jafari, R. Heydari, Study of the removal of metronidazole from aqueous solutions using Electro/Fenton process and graphite and iron electrodes, Yafte, 20 (2018) 41–51.
[14] T.J. Al-Musawi, P. Rajiv, N. Mengelizadeh, F. Sadat Arghavan, D. Balarak, Photocatalytic efficiency of $CuNiFe_2O_4$ nanoparticles loaded on multi-walled carbon nanotubes as a novel photocatalyst for ampicillin degradation, J. Mol. Liq., 337 (2021) 116470, doi: 10.1016/j.molliq.2021.116470.
[15] Y. Ma, Q. Zhou, S. Zhou, W. Wang, J. Jin, J. Xie, A. Li, C. Shuang, A bifunctional adsorbent with high surface area and cation exchange property for synergistic removal of tetracycline and Cu^{2+}, Chem. Eng. J., 258 (2014) 26–33.
[16] H. Sayğılı, F. Güzel, Effective removal of tetracycline from aqueous solution using activated carbon prepared from tomato (*Lycopersicon esculentum* Mill.) industrial processing waste, Ecotoxicol. Environ. Saf., 131 (2016) 22–29.

[17] N. Nasseh, F.S. Arghavan, S. Rodriguez-Couto, A. Hossein Panahi, M. Esmati, T.J. A-Musawi, Preparation of activated carbon@ZnO composite and its application as a novel catalyst in catalytic ozonation process for metronidazole degradation, Adv. Powder Technol., 31 (2020) 875–885.
[18] D. Balarak, F. Mostafapour, H. Azarpira, Adsorption isotherm studies of tetracycline antibiotics from aqueous solutions by maize stalks as a cheap biosorbent, Int. J. Pharm. Technol., 8 (2016) 16664–16675.
[19] W. Liu, H. Xie, J. Zhang, C. Zhang, Sorption removal of cephalexin by HNO_3 and H_2O_2 oxidized activated carbons, Sci. China Chem., 55 (2012) 1959–1967.
[20] A. Almasi, A. Dargahi, M. Mohamadi, H. Biglari, F. Amirian, M. Raei, Removal of Penicillin G by combination of sonolysis and photocatalytic (sonophotocatalytic) process from aqueous solution: process optimization using RSM (Response Surface Methodology), Electron. Physician, 8 (2016) 2878–2887, doi: 10.19082/XX.
[21] I.C. Iakovides, I. Michael-Kordatou, N.F.F. Moreira, A.R. Ribeiro, T. Fernandes, M.F.R. Pereira, O.C. Nunes, C.M. Manaia, A.M.T. Silva, D. Fatta-Kassinos, Continuous ozonation of urban wastewater: removal of antibiotics, antibiotic-resistant Escherichia coli and antibiotic resistance genes and phytotoxicity, Water Res., 159 (2019) 333–347.
[22] F.S. Arghavan, A. Hossein Panahi, N. Nasseh, M. Ghadirian, Adsorption-photocatalytic processes for removal of pentachlorophenol contaminant using FeNi(3)/SiO(2)/ZnO magnetic nanocomposite under simulated solar light irradiation, Environ. Sci. Pollut. Res., 28 (2021) 7462–7475.
[23] N. Nasseh, F.s. Arghavan, N. Daglioglu, A. Asadi, Fabrication of novel magnetic CuS/Fe_3O_4/GO nanocomposite for organic pollutant degradation under visible light irradiation, Environ. Sci. Pollut. Res., (2021) 1–12, doi:10.1007/s11356-020-12066-3.
[24] D. Balarak, F. Mostafapour, E. Bazrafshan, T.A. Saleh, Studies on the adsorption of amoxicillin on multi-wall carbon nanotubes, Water Sci. Technol., 75 (2017) 1599–1606.
[25] N. Nasseh, L. Taghavi, B. Barikbin, M.A. Nasseri, Synthesis and characterizations of a novel $FeNi_3/SiO_2$/CuS magnetic nanocomposite for photocatalytic degradation of tetracycline in simulated wastewater, J. Cleaner Prod., 179 (2018) 42–54.
[26] B. Barikbin, F.S. Arghavan, A. Othmani, A.H. Panahi, N. Nasseh, Degradation of tetracycline in Fenton and heterogeneous Fenton-like processes by using $FeNi_3$ and $FeNi_3/SiO_2$ catalysts, Desal. Water Treat., 200 (2020) 262–274.
[27] M. Khodadadi, T.J. Al-Musawi, M. Kamranifar, M.H. Saghi, A. Hossein Panahi, A comparative study of using barberry stem powder and ash as adsorbents for adsorption of humic acid, Environ. Sci. Pollut. Res., 26 (2019) 26159–26169.
[28] T.J. Al-Musawi, P. Rajiv, N. Mengelizadeh, I.A. Mohammed, D. Balarak, Development of sonophotocatalytic process for degradation of acid orange 7 dye by using titanium dioxide nanoparticles/graphene oxide nanocomposite as a catalyst, J. Environ. Manage., 292 (2021) 112777, doi: 10.1016/j.jenvman.2021.112777.
[29] N. Nasseh, T.J. Al-Musawi, M.R. Miri, S. Rodriguez-Couto, A. Hossein Panahi, A comprehensive study on the application of $FeNi_3$@SiO_2@ZnO magnetic nanocomposites as a novel photo-catalyst for degradation of tamoxifen in the presence of simulated sunlight, Environ. Pollut., 261 (2020) 114127, doi: 10.1016/j.envpol.2020.114127.
[30] T. Xian, L. Di, X. Sun, H. Li, Y. Zhou, H. Yang, Photo-Fenton degradation of AO7 and photocatalytic reduction of Cr(VI) over CQD-decorated $BiFeO_3$ nanoparticles under visible and NIR light irradiation, Nanoscale Res. Lett., 14 (2019) 1–14.
[31] D. Balarak, H. Azarpira, F.K. Mostafapour, Study of the adsorption mechanisms of cephalexin on to Azolla filiculoides, Der Pharma Chemica, 8 (2016) 114–121.
[32] T.J. Al-Musawi, N. Mengelizadeh, O. Al Rawi, D. Balarak, Capacity and modeling of Acid Blue 113 dye adsorption onto Chitosan magnetized by Fe_2O_3 nanoparticles, J. Polym. Environ., (2021), doi: 10.21203/rs.3.rs-334767/v1.
[33] N. Nasseh, F.S. Arghavan, S. Rodriguez-Couto, A. Hossein Panahi, Synthesis of $FeNi_3/SiO_2$/CuS magnetic nanocomposite as a novel adsorbent for Congo Red dye removal, Int. J. Environ. Anal. Chem., (2020) 1–21, doi: 10.1080/03067319.2020.1754810.
[34] S.M. Rahimi, F.S. Arghavan, A. Othmani, N. Nasseh, Magnetically recoverable nickel ferrite coated with CuS nanocomposite for degradation of metronidazole in photocatalytic and photo Fenton like processes, Int. J. Environ. Anal. Chem., (2020) 1–21, doi: 10.1080/03067319.2020.1817420.
[35] M. Forouzesh, A. Ebadi, A. Aghaeinejad-Meybodi, Degradation of metronidazole antibiotic in aqueous medium using activated carbon as a persulfate activator, Sep. Purif. Technol., 210 (2019) 145–151.
[36] F.H. Kamar, A.C. Nechifor, G. Nechifor, T.J. Al-Musawi, A.H. Mohammed, Aqueous phase biosorption of Pb(II), Cu(II), and Cd(II) onto cabbage leaves powder, Int. J. Chem. React. Eng., 15 (2017).
[37] F. Brouers, T.J. Al-Musawi, On the optimal use of isotherm models for the characterization of biosorption of lead onto algae, J. Mol. Liq., 212 (2015) 46–51.
[38] M.H. Alhassani, S.M. Al-Jubouri, H.A. Al-Jendeel, Stabilization of phenol trapped by agricultural waste: a study of the influence of ambient temperature on the adsorbed phenol, Desal. Water Treat., 187 (2020) 266–276.
[39] A. Mohseni-Bandpei, A. Eslami, H. Kazemian, M. Zarrabi, T.J. Al-Musawi, A high density 3-aminopropyltriethoxysilane grafted pumice-derived silica aerogel as an efficient adsorbent for ibuprofen: characterization and optimization of the adsorption data using response surface methodology, Environ. Technol. Innovation, 18 (2020) 100642, doi: 10.1016/j.eti.2020.100642.
[40] J. Wang, G. Liu, T. Li, C. Zhou, Physicochemical studies toward the removal of Zn(II) and Pb(II) ions through adsorption on montmorillonite-supported zero-valent iron nanoparticles, RSC Adv., 5 (2015) 29859–29871.
[41] M. Farzadkia, A. Esrafili, M.A. Baghapour, Y.D. Shahamat, N. Okhovat, Degradation of metronidazole in aqueous solution by nano-ZnO/UV photocatalytic process, Desal. Water Treat., 52 (2014) 4947–4952.
[42] D. Carrales-Alvarado, R. Ocampo-Pérez, R. Leyva-Ramos, J. Rivera-Utrilla, Removal of the antibiotic metronidazole by adsorption on various carbon materials from aqueous phase, J. Colloid Interface Sci., 436 (2014) 276–285.
[43] H.B. Ammar, Sono-Fenton process for metronidazole degradation in aqueous solution: effect of acoustic cavitation and peroxydisulfate anion, Ultrason. Sonochem., 33 (2016) 164–169.
[44] Z. Rahmatinia, M. Rahmatinia, Removal of the metronidazole from aqueous solution by heterogeneous electro-Fenton process using nano-Fe_3O_4, Data Brief, 19 (2018) 2139–2145.
[45] E.M. Kalhori, T.J. Al-Musawi, E. Ghahramani, H. Kazemian, M. Zarrabi, Enhancement of the adsorption capacity of the light-weight expanded clay aggregate surface for the metronidazole antibiotic by coating with MgO nanoparticles: studies on the kinetic, isotherm, and effects of environmental parameters, Chemosphere, 175 (2017) 8–20.
[46] A. Habibi, L.S. Belaroui, A. Bengueddach, A.L. Galindo, C.I.S. Díaz, A. Peña, Adsorption of metronidazole and spiramycin by an Algerian palygorskite. Effect of modification with tin, Microporous Mesoporous Mater., 268 (2018) 293–302.
[47] R. Nosrati, A. Olad, R. Maramifar, Degradation of ampicillin antibiotic in aqueous solution by ZnO/polyaniline nanocomposite as photocatalyst under sunlight irradiation, Environ. Sci. Pollut. Res., 19 (2012) 2291–2299.
[48] N. Nasseh, L. Taghavi, B. Barikbin, M.A. Nasseri, A. Allahresani, $FeNi_3/SiO_2$ magnetic nanocomposite as an efficient and recyclable heterogeneous Fenton-like catalyst for the oxidation of metronidazole in neutral environments: adsorption and degradation studies, Compos. B. Eng., 166 (2018) 328–340.
[49] B. Kakavandi, A. Takdastan, N. Jaafarzadeh, M. Azizi, A. Mirzaei, A. Azari, Application of Fe_3O_4@ C catalyzing heterogeneous UV-Fenton system for tetracycline removal with a focus on optimization by a response surface method, J. Photochem. Photobiol., A, 314 (2016) 178–188.

[50] G. Prados-Joya, M. Sánchez-Polo, J. Rivera-Utrilla, M. Ferro-Garcia, Photodegradation of the antibiotics nitroimidazoles in aqueous solution by ultraviolet radiation, Water Res., 45 (2011) 393–403.
[51] T.J. Al-Musawi, H. Kamani, E. Bazrafshan, A.H. Panahi, M.F. Silva, G. Abi, Optimization the effects of physicochemical parameters on the degradation of cephalexin in sono-Fenton reactor by using Box-Behnken response surface methodology, Catal. Lett., 149 (2019) 1186–1196.
[52] D. Balarak, N. Mengelizadeh, P. Rajiv, K. Chandrika, Photocatalytic degradation of amoxicillin from aqueous solutions by titanium dioxide nanoparticles loaded on graphene oxide, Environ. Sci. Pollut. Res. Int., (2021), doi: 10.1007/s11356-021-13525-1.
[53] P. Rajiv, N. Mengelizadeh, G. McKay, D. Balarak, Photocatalytic degradation of ciprofloxacin with Fe_2O_3 nanoparticles loaded on graphitic carbon nitride: mineralisation, degradation mechanism and toxicity assessment, Int. J Environ. Anal. Chem., (2021) 1–15, doi: 10.1080/03067319.2021.1890059.